Freestanding Borophene and Its Hybrids

Pranay Ranjan, Tumesh Kumar Sahu, Rebti Bhushan, Sharma SRKC Yamijala, Dattatray J. Late, Prashant Kumar, and Ajayan Vinu**

Borophene, an elemental metallic Dirac material is predicted to have unprecedented mechanical and electronic character. Need of substrate and ultrahigh vacuum conditions for deposition of borophene restricts its large-scale applications and significantly hampers the advancement of research on borophene. Herein, a facile and large-scale synthesis of freestanding atomic sheets of borophene through a novel liquid-phase exfoliation and the reduction of borophene oxide is demonstrated. Electron microscopy confirms the presence of β_{12}, X_3, and their intermediate phases of borophene; X-ray photoelectron spectroscopy, and scanning tunneling microscopy, corroborated with density functional theory band structure calculations, validate the phase purity and the metallic nature. Borophene with excellent anchoring capabilities is used for sensing of light, gas, molecules, and strain. Hybrids of borophene as well as that of reduced borophene oxide with other 2D materials are synthesized, and the predicted superior performance in energy storage is explored. The specific capacity of borophene oxide is observed to be ≈4941 mAh g^{-1}, which significantly exceeds that of existing 2D materials and their hybrids. These freestanding borophene materials and their hybrids will create a huge breakthrough in the field of 2D materials and could help to develop future generations of devices and emerging applications.

The emergence of borophene, the lightest elemental anisotropic Dirac material, has been phenomenal (2D materials family shown in Figure S1 in the Supporting Information) owing to its unique mechanical and electronic properties.[1–6] Due to unique bonding behavior of boron, two prominent planar phases of borophene, namely, anisotropic β_{12} having parallel ridges and isotropic hexagonally bonded X_3, have been reported.[7,8] In contrast to the X_3 phase, atomic scale ridges in the β_{12} phase are supposed to enhance thermal stability of borophene sheets. The unique structure and bonding of borophene are responsible for its interesting properties including a low density,[9] a high melting point over 2000 °C, a large bulk modulus of ≈200 GPa,[10,11] a high hardness,[12] and high thermal conductivity.[13,14] Apart from these interesting structural behavior,[15] atomic sheet of borophene is metallic in almost all polymorphs (e.g., boron nanoribbon)[6] which is rare among elemental 2D materials.

For example, graphene and silicene are semimetals and phosphorene is a semiconductor.[2,13] Unlike graphene, which is structurally isotropic in nature, the β_{12} phase of borophene is anisotropic and that in turn is expected to exhibit higher carrier density and mechanical stiffness in preferred direction. Although borophene exhibits these exciting properties, as of now experimental realization of borophene has been achieved via only atomic layer deposition and molecular beam epitaxy (MBE) on the Ag [111] substrate under ultrahigh vacuum condition.[1,3] Recent computational studies proposed that boron in its bulk is not naturally layered and borophene sheet in its pure form (without any holes or protrusions) has been deemed as metastable (higher energy than its bulk).[16,17] In this context, the synthesis of freestanding borophene has not even been thought of to date. It is expected that the discovery of freestanding borophene could open new opportunities for large-scale applications including renewable energy generation and storage as well as in sensors[1–3,18,19] and provides a new platform for realization of novel high-speed low-dissipation devices for electronics application.[20]

We report the discovery of a facile and scalable liquid-phase synthesis of freestanding borophene sheets via sonochemical exfoliation and the role of solvent has been investigated.

Dr. P. Ranjan, T. K. Sahu, R. Bhushan, Prof. P. Kumar
Department of Physics
Indian Institute of Technology Patna
Bihta, Bihar 801106, India
E-mail: prashantkumar@iitp.ac.in

Dr. S. S. Yamijala
Department of Chemistry
University of Rochester
Rochester, NY 14620, USA

The ORCID identification number(s) for the author(s) of this article can be found under https://doi.org/10.1002/adma.201900353.

DOI: 10.1002/adma.201900353

Dr. D. J. Late
National Chemical Laboratory
Pune 411008, India

Prof. P. Kumar
Birck Nanotechnology Centre
Purdue University
West Lafayette, IN 47907, USA

Prof. A. Vinu
Global Innovative Center for Advanced Nanomaterials (GICAN)
Faculty of Engineering and Built Environment
The University of Newcastle
Callaghan, NSW 2308, Australia
E-mail: ajayan.vinu@newcastle.edu.au

Parallelly, the chemical synthesis of borophene oxide via modification in improved Hummer's method[21] and its reduction have been explored to attain freestanding borophene in a scalable manner. To demystify structural ambiguity in freestanding borophene, along with experimental exploration, density functional theory (DFT) band structural calculations for the two prominent phases, namely, β_{12} and X_3, have been carried out. Freestanding borophene sheets have been explored for their potential applications including gas sensing, photosensing, molecular sensing, and strain sensing. In addition, hybrids of freestanding borophene with other 2D materials have been synthesized.

Freestanding borophene with the energetically favorable structure is synthesized via sonochemical exfoliation of boron powder (≈20 µm) in various solvents such as dimethylformamide (DMF), acetone, isopropyl alcohol (IPA), water, and ethylene glycol (EG) (see Figure S4 and Sections S12 and S15 in the Supporting Information for details of borophene sheets attained in various solvents). Acetone and EG as solvents have yielded monolayers within 12 and 20 h, respectively, while other solvents did not yield monolayers. In contrast, water and IPA display fairly good exfoliation down to few monolayers, but the observed sheet sizes are small. The use of DMF, in particular, has resulted in multilayered sheets having ordered crystal structure. While intercalation mediated exfoliation seems to be plausible mechanism for EG and acetone, DMF and water results in surface exfoliation and in IPA fragmentation are dominant over exfoliation. Nature of exfoliation also depends on the polarity of the solvent, available H-bonding, etc.

Freestanding borophene sheets were discovered (for details see Sections S12 and S15 in the Supporting Information) to form in various solvents (as evidenced by transmission electron microscopy (TEM) imaging (Figure S4, Supporting Information). In contrast to other solvents, acetone performs exceedingly well and results in monolayers of borophene (see TEM images in **Figure 1**b and high-resolution transmission electron microscopy (HRTEM) in Figure 1c). The inset image in Figure 1c attests the crystalline nature. Atomic force microscopy (AFM) imaging (Figure 1e) establishes that borophene sheets are varying in thickness and are just a few monolayers (1–10) thick. We obtained AFM visuals which proves the layered nature of the borophene material. The 2D sheet of borophene (Figure 1d) having lateral dimension as large as 1.2 µm has also been observed. In fact, sheets formed are of various thicknesses (as detailed AFM images in Figure S5h–k in the Supporting Information suggest); however, one can isolate either monolayer, bilayer, or even multilayer by centrifugation at adequate speed and time.

We obtained sharp Raman peaks at 130, ≈258, ≈697, and ≈805 cm^{-1} for borophene sheets transferred on a gold coated glass surface (see Figure 1f). In contrast to graphene, borophene is anisotropic and therefore symmetry axes are not identical which will lead to more than one characteristic peaks.

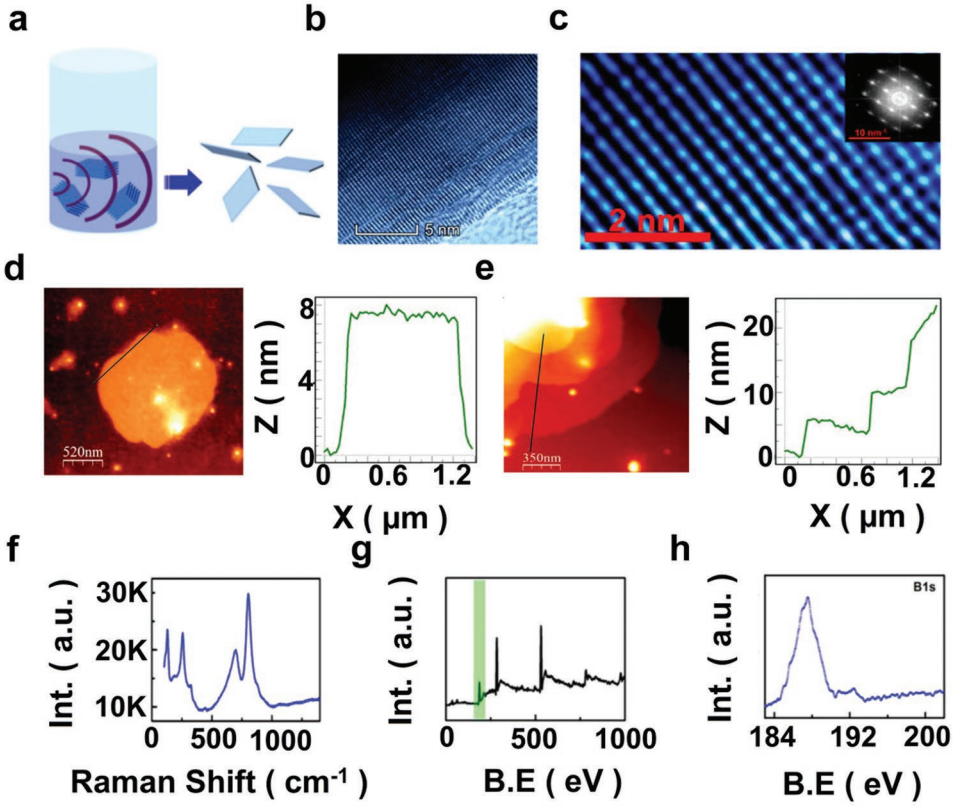

Figure 1. a) Schematic diagram of sonochemical exfoliation synthesis of borophene, b) TEM, and c) HRTEM images (electron diffraction pattern in inset) for borophene synthesized in acetone solvent. d,e) AFM images and corresponding height profiles for typical atomic sheets of borophene at two locations, f) Raman spectrum, g) XPS spectrum (survey) for borophene, and h) short scan XPS B 1s.

Moreover, other than graphene-like defects, atomic displacements toward atomic ridges would contribute to extra Raman peaks. X-ray photoelectron spectroscopy full scan survey (see Figure 1g) carried out on borophene sheet exhibits peaks at 187.1 eV (B 1s), 286.9 eV (C 1s), and 531.3 eV (O 1s) (for details of X-ray photoelectron spectroscopy (XPS) full range spectra see Figure S2 and Section S13 in the Supporting Information). Peaks at 187.1 and 188.2 eV in the short-range spectrum for B 1s (see Figure 1h) correspond to borophene sheet and the peak at 192.5 eV corresponds to the adsorbed oxygen[22] due to exposure to the ambient. However, the oxygen peak is very mild as compared to the reported literature for borophene deposited by molecular beam epitaxy.[3] The presence of oxygen and carbon in the XPS spectrum primarily arises due to airborne impurities and remaining signature of solvents (if any). In order to remove such undesirable peaks owing to the presence of adsorbed O and C and thereby to establish the quality of borophene sheets synthesized by a facile sonochemical route, Ar plasma surface etching was carried out in two steps and XPS spectroscopy was performed at each step (see Figure S2 in the Supporting Information). It is interesting to note that after successive etching steps, each of 15 min duration, O and C indeed diminish and eventually become almost extinct and significant boron peak arises, which proves that the synthesis strategy can yield highly pure borophene which can potentially be employed in devices and sensors.

Selected-area electron diffraction (SAED) pattern for atomic sheets of borophene shows different kinds of patterns for samples synthesized in different solvents. For example, in acetone, hexagonal pattern is observed (Figure S4, Supporting Information). However, for DMF we could visualize overlapping of two kinds of symmetries (namely, twofold and sixfold) which hints at the formation of different structural phases of freestanding borophene. A glimpse of such phases triggers curiosity whether the number of layers would decide and solvents will have role in determining such structures. We observed three distinct symmetry patterns. Overlapped twofold, skewed (signature of strain) sixfold symmetries, and fourfold (rare though) have been observed (see Figure S6a–d in the Supporting Information). It would be crucial therefore to investigate whether these symmetries are available in the same sample or even in the same sheet in freestanding borophene.

Mannix et al.[1] suggest that there are primarily two planar phases of borophene, namely, β_{12} and X_3, out of which X_3 is metastable whereas β_{12} is higher temperature phase. The striped β_{12} phase is rich in carrier density and has excellent Young's modulus (even better than graphene).[23] Band structure calculations of the β_{12} phase for cell and supercell structures exhibit metallic behavior at Γ point (see Figure S6e,f in the Supporting Information). Layer-dependent band structure is observed for both the phases; however, there is a strong dependence for the X_3 phase. Band structures of both β_{12} and X_3 phases confirm metallic nature of borophene (see Figures S6 and S7 in the Supporting Information). However, band structure strongly depends on substrate (for details see Section S14 in the Supporting Information). Metals often possess significant density of state around the Fermi level.[3] In the β_{12} phase, as one can see in the band structure (see Figure S6f in the Supporting Information), out of three prominent bands which crossover the Fermi level, the first two bands arise due to two elliptical hole Fermi sheets which surround the zone center and the third band is attributed to the formation of two semielliptic electron-like Fermi sheets at the Brillouin zone boundary.[24] In the case of the X_3 phase of borophene, however, it was observed that two bands are partially occupied out of which the lower band can be attributed to the twisted quadrilateral hole Fermi sheet at the Γ point and the second partially occupied band arises due to the presence of electron Fermi sheets.

Atoms in borophene sheets were visualized in HRTEM and interatomic distance (also cross-verified by the SAED pattern) was ≈0.25 nm (see Figure 1c), which does not agree with scanning tunneling microscopy (STM) measurements on borophene reported earlier,[1,3] hinting at the observed structure being most likely a Moire's pattern. In order to pin-pointedly resolve this issue, we carried out detailed microscopy of large area and then zoomed-in versions were analyzed. It was really exciting that a part of the same sheet exhibits parallel atomic ridges ≈1 nm apart (signature of the β_{12} phase as can be evidenced in **Figure 2**a) and other part seems to have its ridges diminished (see Figure 2b). In area where we observed atomic ridges, the interatomic distance of boron atoms is ≈2.5 Å for atoms situated in-between the ridges. Also, it should be noted that the number of atoms per unit length on the ridge is higher as compared to that for in-between the ridges. As the distance between the atoms on the ridges is so small, we could not resolve them in our high-resolution TEM images.

Energy of the 2D sheet of boron atoms will have preferentially two minima (which gives rise to two phases, namely, β_{12} and X_3). The intermediate structure obtained in Figure 2b seems to have configuration between β_{12} and X_3. This intermediate metastable structure might have little higher energy than needed for stabilization of β_{12}. The presence of such intermediate phase in freestanding borophene sheets can be attributed to the absence of any lattice (substrate) in contact, which otherwise dictate the geometry of the resulting borophene sheet as reported earlier by Mannix et al.[1] and Feng et al.[3] Thus, in liquid-phase synthesis, final borophene structure will solely be governed by energetics. In fact, out-of plane geometry (e.g., β_{12}) is arising to minimize energy. In-plane geometry in borophene would otherwise give rise to strained lattice. The intermediate phase is supposed to have strain between β_{12} and X_3 phases.

Fast Fourier transform (FFT) carried out in Figure 2a exhibits three parallel rows of dot patterns, out of which the strikingly brighter central row originates from atomic ridges while the other two rows represent atoms situated between the ridges. This observation is an eye-opening proof for the formation of the β_{12} phase in synthesized borophene sheets. FFT carried out in Figure 2b shows a similar pattern. However, when we carried out imaging of another sheet (see Figure 2c), interestingly the part of the image has boron atoms situated ≈2.5 Å apart and other part show narrowly positioned boron atoms ≈1.8 Å apart. This infers that the left part is Moire's pattern and the right part seems to resemble with the X_3 phase. Even though the β_{12} phase shows atoms relatively far apart in-between the ridges as compared to the X_3 phase, yet since ridge portion

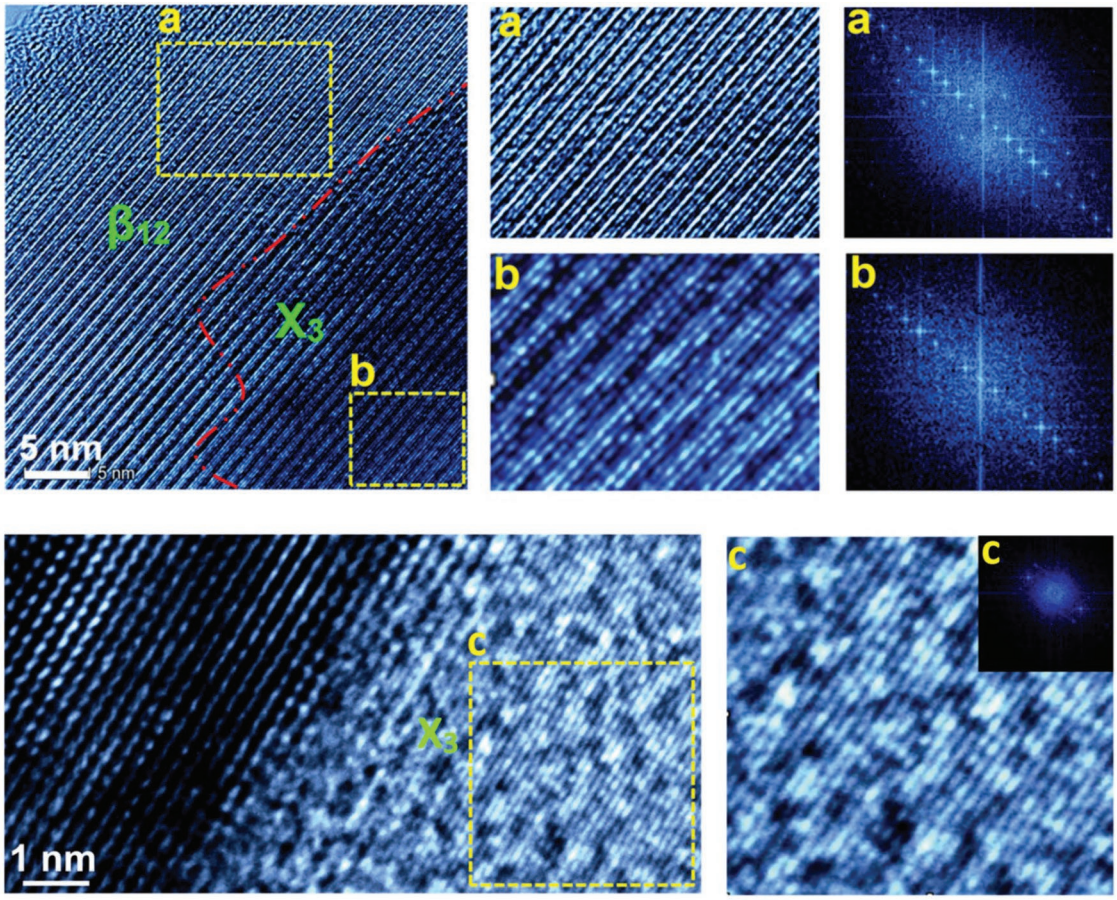

Figure 2. a–c) HRTEM of borophene sheet obtained through sonochemical route in acetone solvent having: a) β_{12}, b) intermediate, and c) X_3-like phase along with their FFT patterns, respectively.

has exceedingly high number density of atoms, the number of atoms per unit area in both the cases would be close. This is in accordance with similar observations by Feng et al.[3] In contrast to sp^3-hybridized graphene, structural anisotropy generated by parallel ridges in the β_{12} phase of borophene will exhibit tremendously strong atomic interactions along the ridge direction, which will eventually lead to surprisingly excellent Young's modulus and electronic carrier density.[1] Even thermal conductivity and refractive indices are also supposed to be distinctly different in two directions. The FFT pattern shown in Figure 2c is drastically different from that for the β_{12} phase shown in Figure 2a. There is a single row in Figure 2c having just three bright dots. These observations of completely distinct features in FFT patterns seem to arise from the two prominent phases. The present investigation thus establishes that both X_3 and β_{12} phases form in freestanding borophene. Such an unambiguous distinction of phases in freestanding borophene has never been reported in the open literature so far.

Oxidation of atomic sheets of borophene seems to be imminent at room temperature and under ambient environment. Also, the adsorption of water molecules on its surfaces is expected. Along with this, grain boundary contribution is anticipated as well in *I–V* measurement.[25] Moreover, two-probe measurement faces contact resistances as well. To our surprise, despite above issues, we observed a metallic behavior in borophene sheets (see **Figure 3**b) in two probe measurement itself (see schematic in Figure 3a). Having glimpse regarding the metallic nature of obtained sheets, we further investigated borophene sheets under STM (see Figure 3c). To our delight, we observed a linear *I–V* behavior in STM and the conductance values of the synthesized sheets were found to be 8.33 nS. It should be noted that the extent of oxidation in our samples is comparatively lower than that for the MBE-deposited borophene layer as evidenced from B 1s peak in XPS results (Figure 1h). It seems that oxidation initiates at edges of borophene sheets, not from surface itself.[3] It would even be more interesting to investigate thermal stability of borophene sheet under ambient environment, which is discussed later.

Graphene strongly interacts with light[26] and has been demonstrated as an excellent material candidate for photodetectors.[27] It was imperative therefore to explore how elemental Dirac material borophene responds when exposed to light. When two-probe device having borophene as an active material was exposed to a white light-emitting diode (LED), we found that borophene is light sensitive and observed that the rise time was faster than the fall time by ≈2.4 times (see Figure 3d). Having appreciably high surface area and in particular parallel boron ridges separated by ≈3 Å, which will electrostatically interact with N atoms, makes borophene very special surface for ammonia sensing.[28] Borophene in fact exhibited excellent sensitivity and selectivity

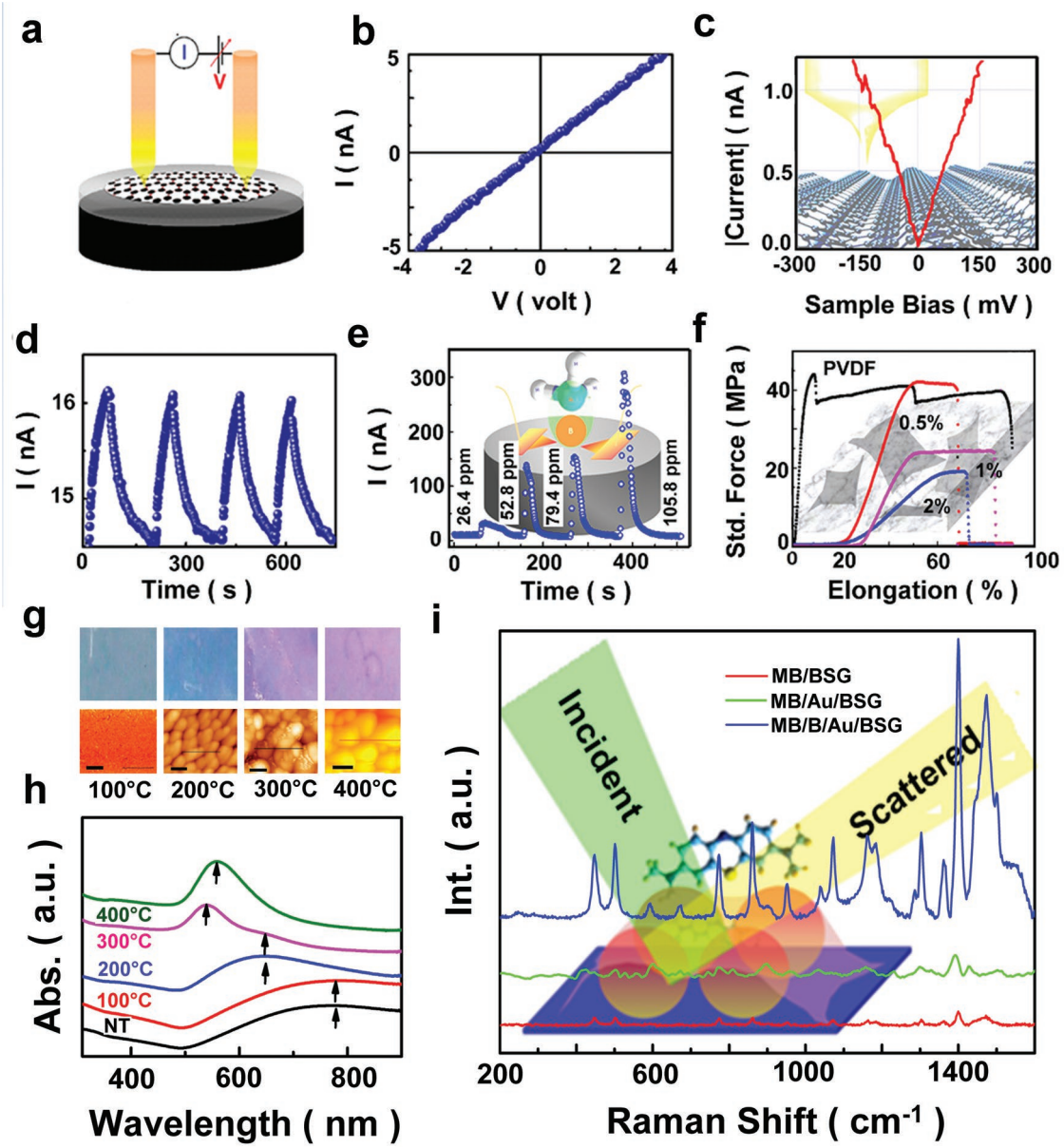

Figure 3. a) Schematic diagram of two-probe *I–V* measurement, b) current–voltage characteristic of borophene sheet, c) STM image (background is image of β_{12} sheet), d) photosensing (white light) by borophene sheet, e) ammonia sensing, f) strain sensing by PVDF sheet with borophene as nanofiller, g) optical and AFM image of Au nanoparticulated thin film sputtered on glass substrate heated at different temperatures, and h) UV–vis spectra for films shown in (g), and i) molecular sensing by SERS: Raman spectra of methylene blue dye on borosilicate glass, Au/borosilicate glass, and borophene/Au/borosilicate glass.

(volatile organic compounds, e.g., acetone and ethanol did not respond). Typical response time of freestanding borophene was observed as ≈7 s for 79.4 ppm (see Figure 3e).

Apart from possessing attributes of graphene (i.e., atomically flat, optically transparent, and high electronic mobility[29]), borophene is mechanically anisotropic due to atomic ridges superior Young's modulus than graphene along its ridges.[10] As compared to poly(vinylidene difluoride) (PVDF) that shows ≈8% elongation at ≈42 MPa, PVDF–borophene nanocomposite (0.5 wt% of nanofiller) exhibits 50% elongation at 40 MPa and 1 wt% nanofilled PVDF exhibits 60% elongation at ≈20 MPa (see Figure 3f). This establishes mechanical strengthening of the polymer by borophene. Further when nanofiller wt% was increased, degraded elastic nature of nanocomposite was observed, which possibly arises due to clustering of borophene sheets. Molecular sensing of methylene blue for ≈10 ppm has been demonstrated employing borophene sheets transferred on gold coated glass via surface-enhanced Raman scattering (SERS) (see Section S16 in the Supporting Information).

As sonochemical exfoliation has its own limitations regarding yield of material and therefore, in order to explore scalable applications of freestanding borophene, another synthesis strategy was developed. A suitable adaptation of the improved Hummer's method[21,30] was employed to synthesize borophene

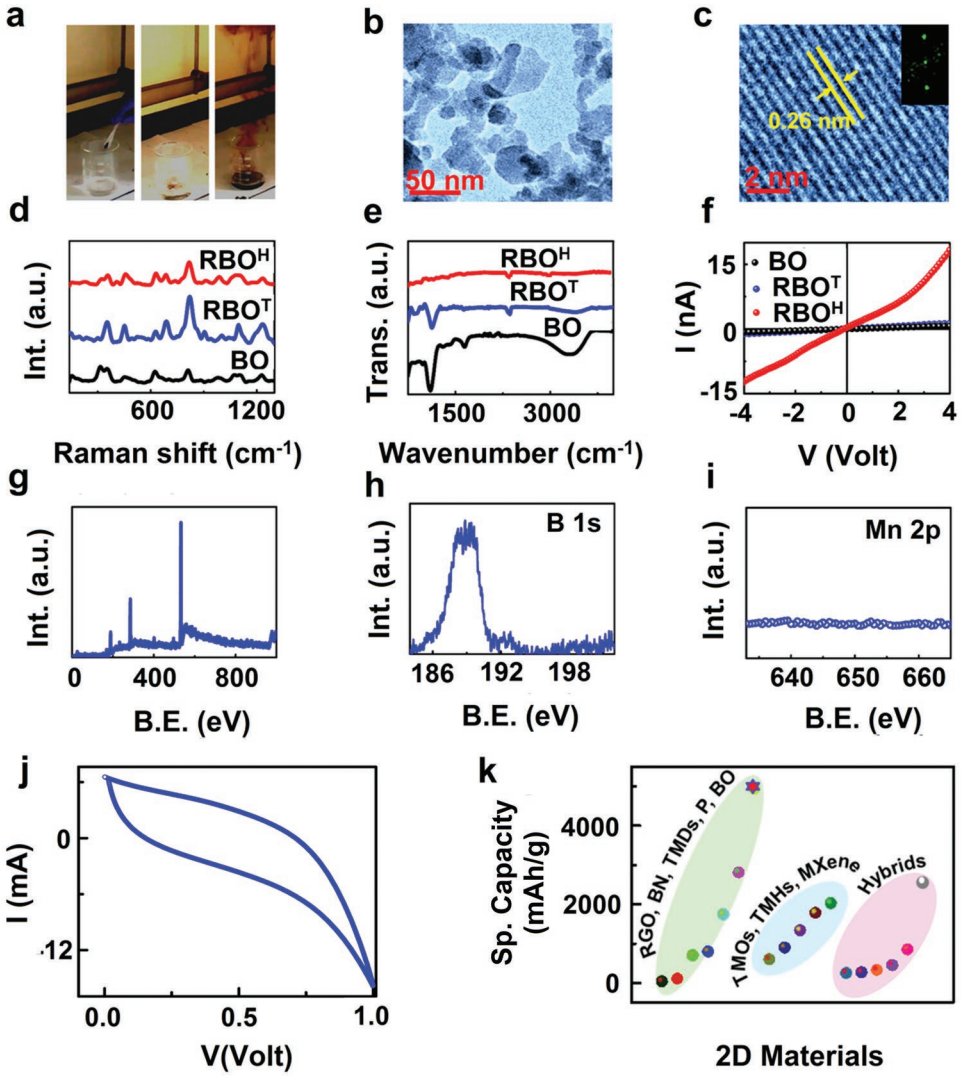

Figure 4. a) Camera image for chemical synthesis of BO. b) TEM image of the BO sheets. c) HTREM of the BO sheets. d,e) Comparison of Raman (d) and FTIR (e) spectra of BO and RBO using hydrothermal and thermal reduction. f) *I–V* characteristics of samples in (d). g–i) XPS spectrum (survey) for BO (g), short scan B 1s (h), and short scan Mn 2p (i). j) Electrochemical *C–V* scans for BO and k) schematic diagram comparing specific capacity of BO with existing 2D materials and their hybrids. Results from the experiments presented here are plotted alongside results replotted from data originally presented in ref. [26].

oxide,[31] which was then reduced to attain reduced borophene oxide (RBO) (for details see Sections S12 and S18 in the Supporting Information). Precooling protocol has been followed to pre-empt any explosion.[21] As soon as B + $KMnO_4$ solid mixture is poured in acid mixture, ignition was evidenced and instantly it caught fire which eventually turned into brown thick smoke which was collected (**Figure 4**a; for details see Figure S8 in in the Supporting Information). Along with the fluffy fibrous material obtained from the thick smoke, materials inside the beaker were purified and analyzed as well. Synthesized material is few layer thin atomic sheets with lateral dimension 20–100 nm (see Figure 4b). As is apparent from HRTEM, material is highly crystalline with an interplanar distance of 2.6 Å (see Figure 4c).

In order to reduce the oxygen functionalities at the surface and edges, we carried out reduction via thermal as well as hydrothermal treatment and monitored the reduction employing Raman as well as Fourier transform infra-red (FTIR) spectroscopy and *I–V* measurements (see Figure 4d–f). Interestingly, upon hydrothermal reduction, characteristic Raman peaks of borophene (attained via sonochemical synthesis) at ≈630, ≈680, ≈800, and 910 cm^{-1} have been observed to be restored which were either absent or highly shifted in BO. A detailed analysis of theoretical Raman modes is given in Section S15 and Table S1 in the Supporting Information). While B—OH peak centered ≈ 3400 cm^{-1} and B—O peak centered ≈1125 cm^{-1} in FTIR spectrum got partially reduced upon thermal reduction, hydrothermal treatment completely removed any signature of surface functionalities as can be evidenced in Figure 4e. While thermal treatment of BO resulted in marginal change in conductance from 0.16 to 0.35 nS, hydrothermal treatment in contrast resulted in significant rise in conductance from 0.16 to 4.5 nS, which attests to efficient reduction and hence the formation of RBO (see Figure 4f).

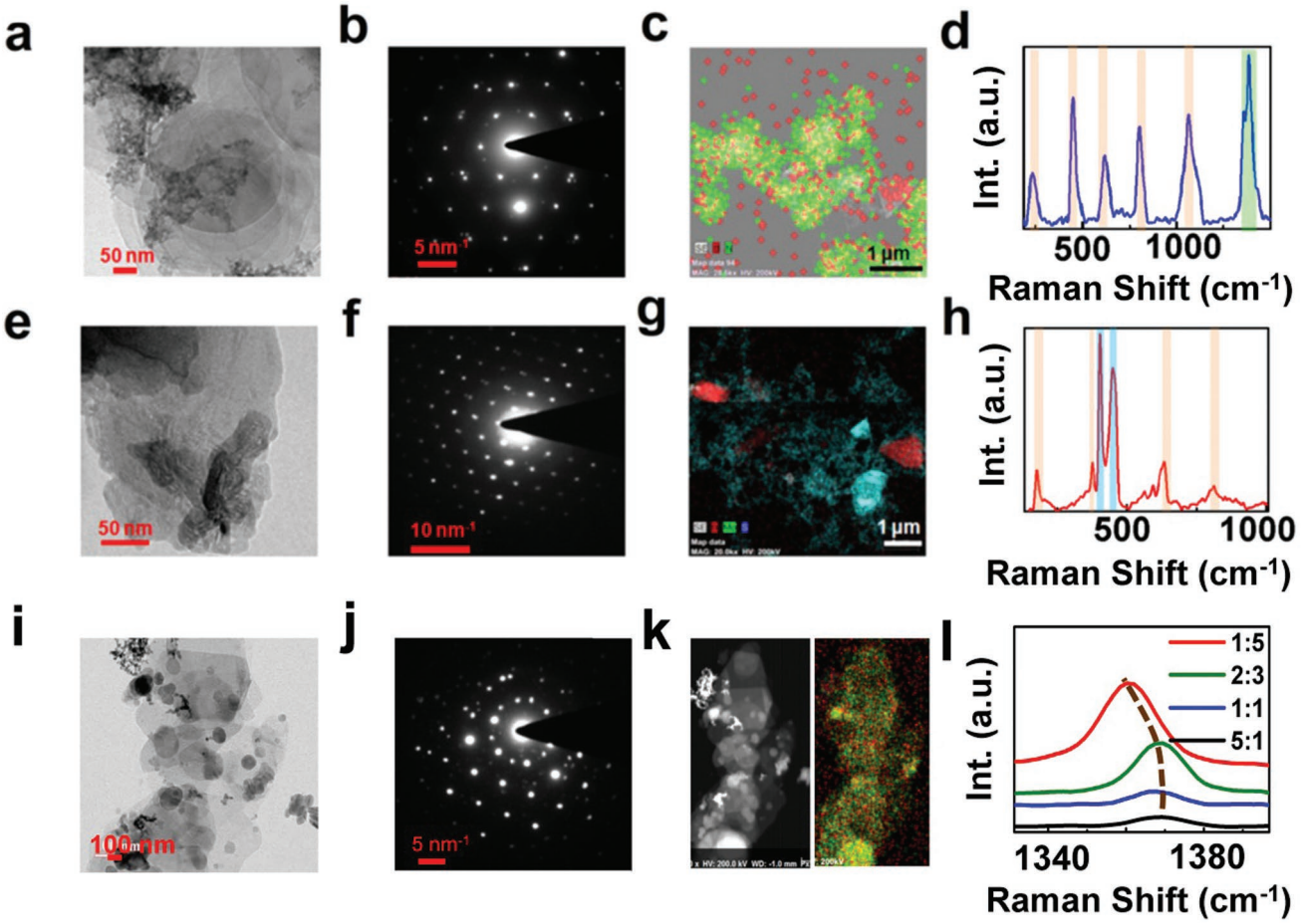

Figure 5. a) TEM, b) HRTEM, c) elemental mapping, and d) Raman spectra of B/BN hybrid nanosystem. e) TEM, f) HRTEM, g) elemental mapping, and h) Raman spectra of B–MoS_2 hybrid nanosystem. i) TEM, j) HRTEM, k) Elemental mapping, and l) Raman spectra of RBO–BN hybrid nanosystems with different ratios of components.

XPS spectroscopy further proves the phase purity of the sample as we obtained characteristic peaks in survey (see Figure 4g), and interestingly B 1s peak positioned at BE ≈189 eV approves the formation of borophene (see Figure 4h). Moreover, we could not find any trace of remnant MnO_2 as confirmed by the absence of Mn 2p peak in XPS (see Figure 4i). As synthesized BO was electrochemically tested (see Figure 4j) and interestingly its specific capacity is ≈4941 mAh g^{-1} which by any means is superior over existing 2D materials (refer Figure 4k) and their hybrids, revealing its possible applications in supercapacitors.[34]

Bandgap engineering has been a huge drive for research on hybrid nanomaterials, and the electronic conductivity, refractive index, thermal conductivity, mechanical strength and other physical behaviors can be engineered through hybridization.[32] As graphene–BN interfaces have been demonstrated for enhanced electronic mobility and optical waveguide in the THz range of frequency,[33] the exploration of borophene-BN interface becomes urgent. Even though vulnerability of borophene toward oxidation at elevated temperature has not yet been established, it is anticipated that it would be oxidized as the atomic sheet being metallic. In this context therefore its hybridization with BN (T_{melt} ≈ 3000 °C) can be advantageous, which will exploit borophene character for sensitivity and BN character for thermal robustness. In order to attain practical realization of such niche applications, we investigated structural fidelity via thermogravimetric analysis (TGA) and also followed it through electrical characterizations (*I*–*V*) and found that borophene sheets get oxidized above 673 K (see Figure S9 in the Supporting Information). In order to render it robustness under extreme thermal conditions, therefore sonochemically exfoliated borophene was blended (by cosonication of the supernatants of individual dispersions) with BN and MoS_2 (which themselves were synthesized by sonochemical route; see details in **Figure 5**a–h). Thermal and microwave stability as well as fire retardant behavior has been investigated (see Section S17 in the Supporting Information). Also, chemically synthesized RBO was blended with BN (see Figure 5i–l and details in Figure S10 and Section S18 in the Supporting Information). In all the hybrid nanosystems, we attained overlap region between two component materials sheets (as apparent from elemental mapping), where the hybridization of P_z orbitals are expected to take place. Interestingly, BN Raman peak shifts toward higher wave number when borophene content was increased in the hybrid.

In conclusion, the myth that borophene 2D sheet cannot form without the support of substrates which is believed to have predominant role in the crystallization of flat sheet of

boron has been broken. Freestanding borophene (β_{12}, X_3, and intermediate phases) with monolayer as well as few layer sheets have experimentally been realized for the first time via facile sonochemical exfoliation (acetone was found excellent solvent) as well as through reduction of BO which itself was synthesized for the first time. The extent of oxidation in freestanding borophene is not alarming rather minimal (as XPS suggests); moreover, when diagnosed in TGA, borophene sheet oxidizes above 673 K in air; it is therefore practically safe to be employed in devices working under ambient conditions. Metallic nature of borophene sheets has been established by STM measurement and supported by DFT band structure calculations as well. Freestanding borophene has been demonstrated for its applications for gas, photo, strain, and SERS-based molecular sensing. Hybrids of borophene (B–BN, B–MoS_2, and RBO–BN) have been synthesized. In contrast to atomic layer deposition and MBE, sonochemical as well as chemical synthesis yield freestanding borophene sheets in a scalable manner and is bound to expand the horizon of applications.

Supporting Information

Supporting Information is available from the Wiley Online Library or from the author.

Acknowledgements

T.K.S. and R.B. contributed equally to this work. The authors acknowledge Department of Science and Technology, Govt. of India, for Research grant under Ramanujan Fellowship (Sanction No. SB/S2/RJN-205/2014). The authors would also like to acknowledge Ajay D. Thakur for fruitful discussion related to the chemical synthesis of BO and Indian Institute of Technology Patna for providing research facilities. P.R. would like to acknowledge VITM for their research support. P.K. conceived the idea. P.R. carried out synthesis of freestanding borophene via physical and chemical routes and explored its applications. T.K.S. synthesized hybrids of borophene with other 2D materials and their characterization. R.B. carried out electrochemical measurements. D.J.L. helped with SERS application. S.R.K.C.Y. carried out band structure calculations for borophene. P.K. discussed electrochemical results with A.V. and then wrote the manuscript. A.V thanks Australian Research Council (DP 170104478 and DP 150104828) and the University of Newcastle for the funding.

Conflict of Interest

The authors declare no conflict of interest.

Keywords

2D materials hybrids, freestanding borophene, liquid-phase exfoliation, reduced borophene oxide, scalable synthesis

Received: January 16, 2019
Revised: March 14, 2019
Published online: May 1, 2019

[1] A. J. Mannix, X. F. Zhou, B. Kiraly, J. D. Wood, D. Alducin, B. D. Myers, X. Liu, B. L. Fisher, U. Santiago, J. R. Guest, M. J. Yacaman, A. Ponce, A. R. Oganov, M. C. Hersam, N. P. Guisinger, *Science* **2015**, *350*, 1513.
[2] A. J. Mannix, Z. Zhang, N. P. Guisinger, B. I. Yakobson, M. C. Hersam, *Nat. Nanotechnol.* **2018**, *13*, 444.
[3] B. Feng, J. Zhang, Q. Zhong, W. Li, S. Li, H. Li, P. Cheng, S. Meng, L. Chen, K. Wu, *Nat. Chem.* **2016**, *8*, 563.
[4] B. Feng, J. Zhang, S. Ito, M. Arita, C. Cheng, L. Chen, K. Wu, F. Komori, O. Sugino, K. Miyamoto, T. Okuda, S. Meng, I. Matsuda, *Adv. Mater.* **2018**, *30*, 2.
[5] P. Kumar, J. Liu, P. Ranjan, Y. Hu, S. S. R. K. C. Yamijala, S. K. Pati, J. Irduyaraj, G. J. Cheng, *Small.* **2018**, *14*, 1703346.
[6] Q. Zhong, L. Kong, J. Gou, W. Li, S. Sheng, S. Yang, P. Cheng, H. Li, K. Wu, L. Chen, *Phys. Rev. Mater.* **2017**, *1*, 021001.
[7] X. Wu, J. Dai, Y. Zhao, Z. Zhuo, J. Yang, X. C. Zheng, *ACS Nano* **2012**, *6*, 7443.
[8] G. P. Campbell, A. J. Mannix, J. D. Emery, T. L. Lee, N. P. Guisinger, M. C. Hersam, M. J. Bedzyk, *Nano Lett.* **2018**, *18*, 2816.
[9] Q. Weng, G. Li, X. Feng, K. Nielsch, D. Golberg, O. G. Schmidt, *Adv. Mater.* **2018**, *30*, 1801600.
[10] B. Mortazavi, O. Rahaman, A. Dianat, T. Rabczuk, *Phys. Chem. Chem. Phys.* **2016**, *18*, 27405.
[11] R. Pekoz, M. Konuk, M. E. Kilic, E. Durgun, *ACS Omega* **2018**, *3*, 1815.
[12] B. Peng, H. Zhang, H. Shao, Z. Ning, Y. Xu, G. Ni, H. Lu, D. W. Zhang, H. Zhu, *Mater. Res. Lett.* **2017**, *5*, 399.
[13] H. Zhou, Y. Cai, G. Zhang, Y. W. Zhang, *npj 2D Mater. Appl.* **2017**, *1*.
[14] D. Li, J. He, G. Ding, Q. Tang, Y. Ying, J. He, C. Zhou, Y. Liu, C. Feng, Q. Sun, H. Zhou, P. Zhou, G. Zhang, *Adv. Funct. Mater.* **2018**, *28*, 1801685.
[15] Z. Zhang, E. S. Penev, B. I. Yakobson, *Chem. Soc. Rev.* **2017**, *46*, 6746.
[16] X. Sun, X. Liu, J. Yin, J. Yu, Y. Li, Y. Hang, X. Zhou, M. Yu, J. Li, G. Tai, W. Guo, *Adv. Funct. Mater.* **2017**, *27*, 1603300.
[17] Q. Zhong, J. Zhang, P. Cheng, B. Feng, W. Li, S. Sheng, H. Li, S. Meng, L. Chen, K. Wu, *J. Phys.: Condens. Matter* **2017**, *29*, 095002.
[18] L. Kong, K. Wu, L. Chen, *Front. Phys.* **2018**, *13*, 138105.
[19] B. Feng, J. Zhang, R.-Y. Liu, T. Iimori, C. Lian, H. Li, L. Chen, K. Wu, S. Meng, F. Komori, I. Matsuda, *Phys. Rev. B* **2016**, *94*, 041408.
[20] B. Feng, O. Sugino, R.-Y. Liu, J. Zhang, R. Yukawa, M. Kawamura, T. Iimori, H. Kim, Y. Hasegawa, H. Li, L. Chen, K. Wu, H. Kumigashira, F. Komori, T.-C. Chiang, S. Meng, I. Matsuda, *Phys. Rev. Lett.* **2017**, *118*, 096401.
[21] P. Ranjan, S. Agarwal, A. Sinha, T. R. Rao, J. Balakrishnan, *Sci. Rep.* **2018**, *8*, 12007.
[22] C. W. Ong, H. Huang, *J. Appl. Phys.* **2004**, *95*, 3527.
[23] C. Lee, X. Wei, J. W. Kysar, Hone, *Science* **2008**, *321*, 385.
[24] M. Gao, Q. Z. Li, X. W. Yan, J. Wang, *Phys. Rev. B* **2017**, *95*, 1.
[25] A. W. Tsen, L. Brown, M. P. Levendorf, F. Ghahari, P. Y. Huang, R. W. Havener, C. S. R. Vargas, D. A. Muller, P. Kim, J. Park, *Science* **2012**, *336*, 1143.
[26] T. Higuchi, C. Heide, K. Ullmann, H. B. Weber, P. Hommelhoff, *Nature* **2017**, *550*, 224.
[27] C. H. Liu, Y. C. Chang, T. B. Norris, Z. Zhong, *Nat. Nanotechnol.* **2014**, *9*, 273.
[28] V. Shukla, J. Wärnå, N. K. Jena, A. Grigoriev, R. Ahuja, *J. Phys. Chem. C* **2017**, *121*, 26869.
[29] T. Ramanathan, A. A. Abdala, S. Stankovich, D. A. Dikin, M. Herrera-Alonso, R. D. Piner, D. H. Adamson, H. C. Schniepp, X. Chen, R. S. Ruoff, S. T. Nguyen, I. A. Aksay, R. K. Prud'Homme, L. C. Brinson, *Nat. Nanotechnol.* **2008**, *3*, 327.
[30] D. C. Marcano, D. V. Kosynkin, J. M. Berlin, A. Sinitskii, Z. Sun, A. Slesarev, L. B. Alemany, W. Lu, J. M. Tour, *ACS Nano* **2010**, *4*, 4806.
[31] C. Zhong, W. Wu, J. He, G. Ding, Y. Liu, D. Li, S. A. Yang, G. Zhang, *Nanoscale* **2019**, *11*, 2468.
[32] J. Wan, S. D. Lacey, J. Dai, B. BAo, M. S. Fuhrer, L. Hu, *Chem. Soc. Rev.* **2016**, *45*, 6742.
[33] T. Low, P. Avouris, *ACS Nano* **2014**, *8*, 1086.
[34] K. S. Kumar, N. Choudhary, Y. Jung, J. Thomas, *ACS Energy Lett.* **2018**, *3*, 482.